Journal of Quantitative Spectroscopy & Radiative Transfer 246 (2020) 106911

Contents lists available at ScienceDirect

Journal of Quantitative Spectroscopy & Radiative Transfer

journal homepage: www.elsevier.com/locate/jqsrt

Infrared transmission spectra of hot ammonia in the 4800–9000 cm^{-1} region

Christopher A. Beale[a,1], Andy Wong[b,1], Peter Bernath[a,b,1,*]

[a] Department of Ocean, Earth and Atmospheric Sciences, Old Dominion University, Norfolk, VA, United States
[b] Department of Chemistry and Biochemistry, Old Dominion University, Norfolk, VA, United States

ARTICLE INFO

Article history:
Received 24 January 2020
Revised 17 February 2020
Accepted 17 February 2020
Available online 19 February 2020

ABSTRACT

Line lists of ammonia (NH_3) are presented at elevated temperatures (293–900 K at 100 K intervals) for the 4800–9000 cm^{-1} region at pressures of 10 Torr and 100 Torr. This region includes a number of overtone, combination and related hot bands. The line lists were obtained by Fourier transform transmission spectroscopy and include calibrated line positions and intensities as well as estimates of empirical lower state energies by comparison of line intensities at different temperatures. These line lists are relevant to the study of the atmospheres of exoplanets and brown dwarfs.

1. Introduction

The ammonia (NH_3) molecule is important in the study of a number of planetary atmospheres and other astronomical objects. On Earth, the sources of NH_3 are primarily from agriculture and from biomass burning [1]. NH_3 in the atmosphere has a negative effect on nutrient balances in plants [2] and leads to increased nucleation of atmospheric aerosols [3]. In space, NH_3 has been detected in many sources, including molecular clouds [4,5], star forming regions [6] as well as in brown dwarfs [7] and the atmospheres of Solar System bodies such as Jupiter [8], Saturn [9] and Titan [10].

Ammonia has been observed in the atmospheres of brown dwarfs by infrared spectroscopy [7] and may be present in the atmospheres of exoplanets [11]. Brown dwarfs are substellar objects without sufficient mass to fuse hydrogen in their cores but are over the mass threshold to fuse deuterium [12]. As such, brown dwarfs are cooler than the coolest stars and the atmospheres of T-type brown dwarfs have temperatures at which polyatomic molecules such as CH_4 and NH_3 are present [13].

Ammonia has a trigonal pyramid structure having C_{3v} symmetry. Of the six fundamental modes of vibration, two are doubly degenerate resulting in four fundamental vibrational frequencies. These are the symmetric stretch at 3336.2 cm^{-1} (ν_1, a_1), the symmetric bend at 932.5 cm^{-1} (ν_2, a_1), the antisymmetric stretch at 3443.6 cm^{-1} (ν_3, e) and the antisymmetric bend at 1626.1 cm^{-1} (ν_4, e). The spectrum of ammonia has been studied numerous times. Experimental studies in the mid and near infrared include, for example, line lists in the 2 μm [14], 2.3 μm [15] and 3 μm [16] regions as well as studies that obtained temperature dependent line lists and empirical lower state energies in the 740–2100 cm^{-1} [17] 1650–4000 cm^{-1} [18] and 2400–5500 cm^{-1} [19] regions.

The most extensive line lists for ammonia have been obtained by theoretical methods. Ro-vibrational calculations from Huang et al. [20,21] used an experimentally refined potential energy surface to obtain energies and quantum assignments in the mid infrared, including identification of new vibrational bands for $^{14}NH_3$, $^{15}NH_3$ and $^{14}ND_3$. BYTe, a comprehensive *ab initio* line list for NH_3 includes over 1.1 billion transitions and can be used at temperatures of up to 1500 K [22]. The latest ExoMol line list for ammonia (CoYuTe) has 16.9 billion vibration-rotation lines and is also intended for applications up to 1500 K [23].

The HITRAN 2016 database [24] is the most widely used database for ammonia and includes quantum number assignments. The HITRAN database is intended to be used for remote sensing applications for the Earth's atmosphere and therefore lacks many hot bands which are needed for spectra of objects at high temperatures such as brown dwarfs and exoplanets.

The work reported here is on the measurement of the ammonia transmission spectra in the 4800–8800 cm^{-1} region at temperatures of 293–900 K at pressures of 10 Torr and 100 Torr.

* Corresponding author at: Department of Chemistry and Biochemistry, Old Dominion University, Norfolk, VA, United States.
E-mail address: pbernath@odu.edu (P. Bernath).
[1] Current address: Department of Civil and Environmental Engineering, Princeton University, Princeton, NJ, United States.

https://doi.org/10.1016/j.jqsrt.2020.106911
0022-4073/

Table 1
Experimental conditions for NH3 spectra.

Parameter	Value
Spectral region (cm^{-1})	4800–9000
Detector	InSb
Beamsplitter	CaF_2
Spectrometer windows	CaF_2
Lens	CaF_2
Filters	Si, 2 μm blue pass
Scans	300
Resolution (cm^{-1})	0.01
Pathlength (cm)	50.8
NH_3 pressure (Torr)	10/100
Zerofilling factor	x 16

2. Experimental

The 2400–5500 cm^{-1} region contains the ν_1 and ν_3 modes, as well as several combination and overtone bands [19]. The 4800–9000 cm^{-1} region contains no fundamental modes, only combinations or overtones of the four fundamental frequencies. The intensity of transitions in this region is generally lower than those in the 2400–5500 cm^{-1} region. In order to compensate for the varied band intensities, the spectra in this higher wavenumber region were recorded at two pressures, 10 Torr and 100 Torr.

Increased pressure results in more of the sample gas and therefore stronger absorption by the lines. However, pressure broadening increases the line width. In this higher wavenumber region, the 100 Torr spectra allow the weaker lines to be visible at the expense of increased line widths. For a molecule such as ammonia, which has a congested spectrum, increased line widths can result in blended lines which increases the uncertainty in the position and intensity of individual lines. In our previous work in the 2400–5500 cm^{-1} region, substantial decomposition was found at 973 K so the highest temperature used in the present work was 900 K. NH_3 transmission spectra were recorded at 7 sample temperatures: 293, 400, 500, 600, 700, 800 and 900 K., and the experimental conditions are summarized in Table 1.

Transmission spectra were obtained for ammonia using the same method and experimental setup as was used for the 2400–5500 cm^{-1} region of ammonia in our previous work [19], which is based on the method used for CH_4 [25]. Absorption spectra were recorded using a 200 W tungsten halogen lamp as a light source, with ammonia in the cell (A_{ab}) and without ammonia present in the cell (A_{ref}). For higher temperatures, the emission signal from the sample and the cell becomes strong enough that it must be accounted for. Therefore, emission spectra with the lamp off are recorded with ammonia in the cell (B_{em}) and without ammonia (B_{ref}). The transmission spectrum is then given by

$$\tau = \frac{A_{ab} - B_{em}}{A_{ref} - B_{ref}}$$

Using Carleer's WSpectra [26], lines were picked from 4800–9000 cm^{-1} for the 10 Torr spectra and from 5500–9000 cm^{-1} for the 100 Torr spectra. The combination band around 5300 cm^{-1} was not included for line selection for the higher-pressure spectra as this band was at the edge of the region and suffers from low signal-to-noise (Fig. 1). The noise for most of this region is

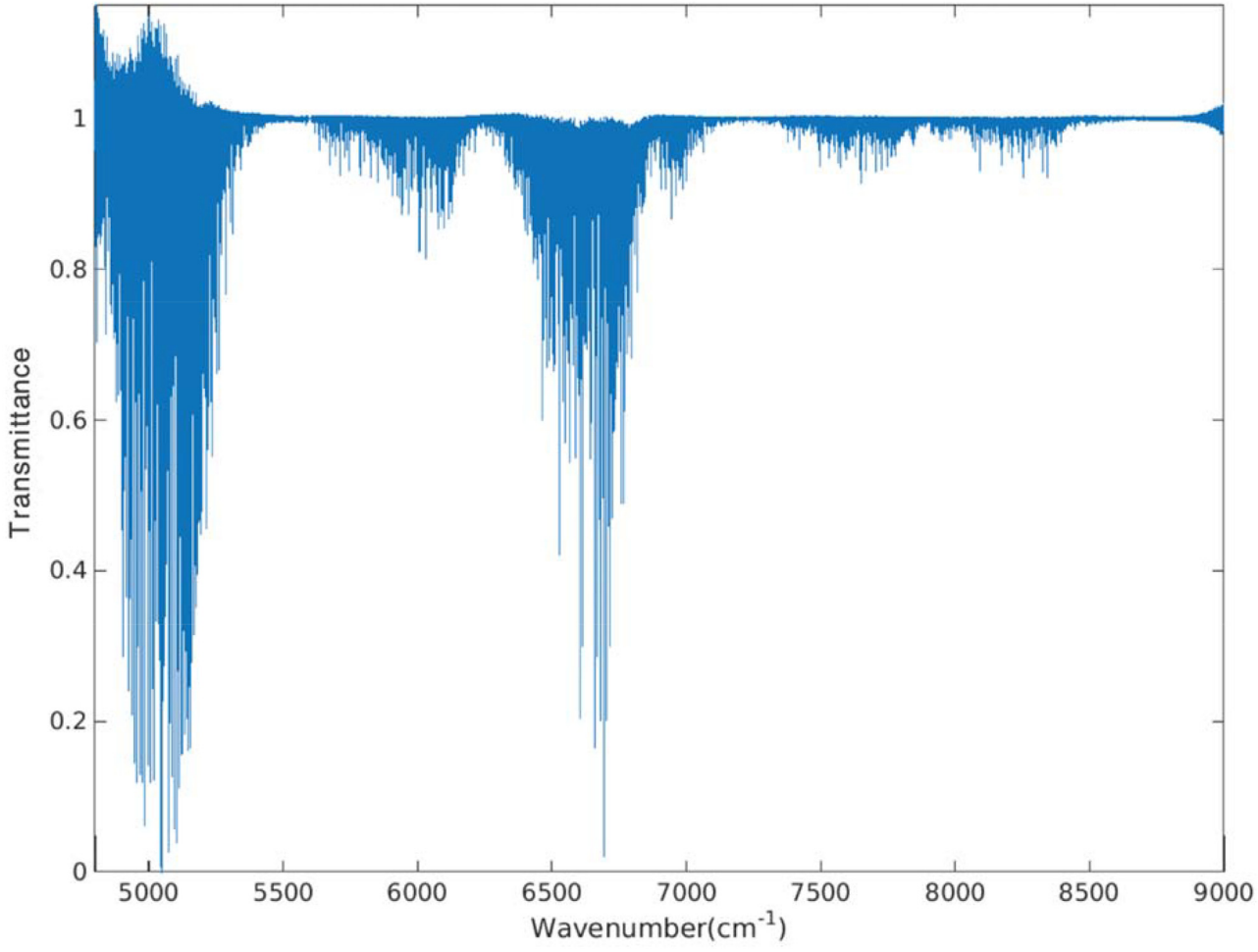

Fig. 1. Overview ammonia transmission spectrum at 700 K with 100 Torr pressure in a 50.8 cm long cell.

Table 2
Calibration factors for experimental line positions (Pos.) and intensities (Int.) for each temperature and pressure.

Temperature (K)	10 Torr Pos. Calib. Factor	10 Torr Int. Calib. Factor (x 10^{-21} cm/molecule)	100 Torr Pos. Calib. Factor	100 Torr Int. Calib. Factor (x 10^{-21} cm/molecule)
293	1.000000081	2.14	1.000000094	1.01
400	1.000000083	2.78	1.000000096	0.99
500	1.000000125	3.83	1.000000100	1.42
600	1.000000116	3.53	1.000000063	1.30
700	1.000000115	4.56	1.000000090	1.29
800	1.000000065	7.18	1.000000099	1.41
900	1.000000109	3.10	1.000000083	1.51

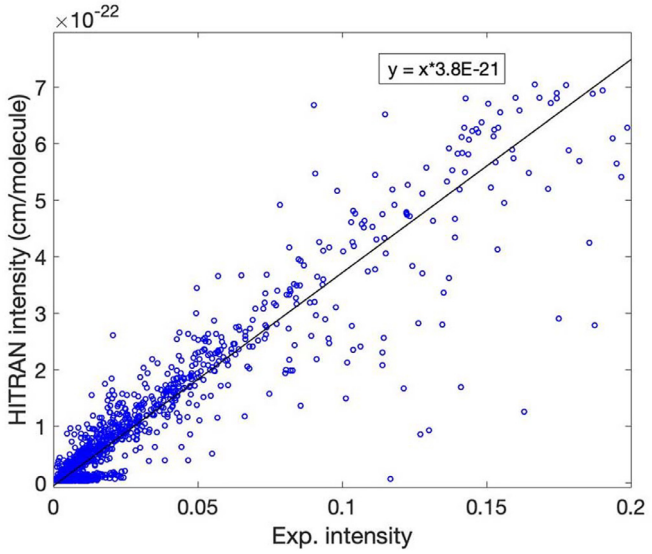

Fig. 2. Intensity calibration plot for 500 K at 10 Torr. The calibration factor is the value of the trend line, which for example with this calibration is 3.8 × 10^{-21}. The x-axis units are cm^{-1}.

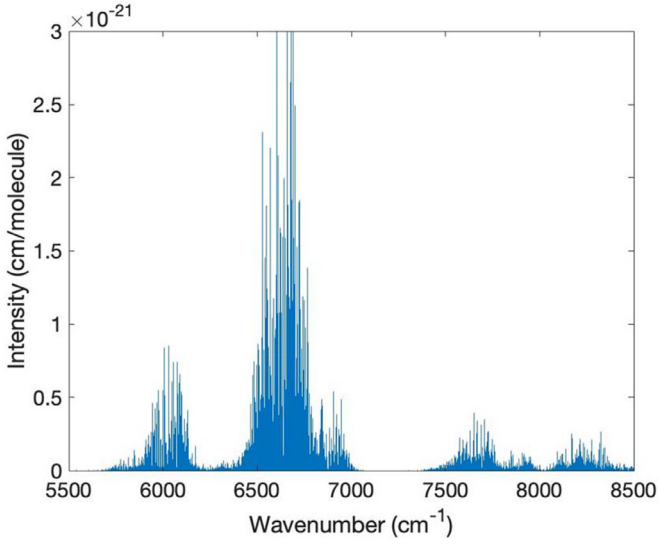

Fig. 3. Spectrum of NH_3 at a temperature of 293 K and pressure of 10 Torr. This spectrum has been calibrated for both wavenumber and intensity.

under ±0.2%, but at 5200 cm^{-1} and below, the noise ranges up to ±15%, which combined with high pressure, results in lines with poorly determined line positions and intensities. Since this band is relatively strong, the line positions and intensities from the 10 Torr spectra as well as from the edge of the 2400–5500 cm^{-1} spectra [19] are sufficient to provide a suitable line list for this band.

Line positions are calibrated by comparison with NH_3 lines found in HITRAN that are both strong and isolated. Line intensities are obtained using WSpectra, which applies a non-linear least squares fit, line-by-line, using a Voigt profile. The output of this fit is the raw line positions and intensities (in cm^{-1} units) which are then calibrated with HITRAN values. The line positions in each spectrum are multiplied by calibration factors given in Table 2. Similar to the calibration of line positions, calibration of line intensities is done by comparison to HITRAN as shown in Fig. 2. A summary of the intensity calibration factors is provided in Table 2 and these factors are used to give the experimental intensities in useful units. Although the spectrum with 100 Torr of NH_3 has pressure shifts, the wavenumber calibration with HITRAN corrects for these shifts on average.

A sample of these spectra (293 K at 10 Torr) is presented in Fig. 3. Once calibrated, the line intensities should be the same regardless of pressure. As a check, the calibrated intensity of a spectrum recorded at 10 Torr against is plotted against that of a spectrum recorded at 100 Torr (Fig. 4). The numbers of lines measured at each temperature are given in Table 3.

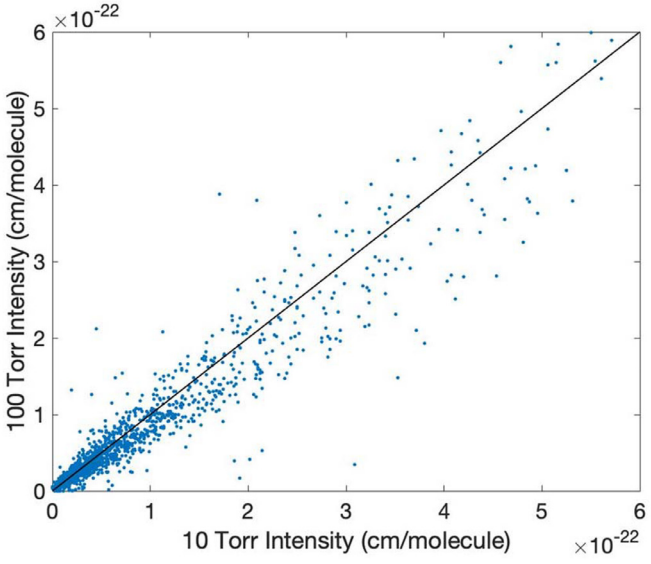

Fig. 4. Comparison of calibrated intensities from at pressures of 10 Torr (x-axis) and 100 Torr (y-axis) at 293 K and a 1:1 trend line.

3. Results and discussion

Once a calibrated line list was obtained for each temperature and pressure, empirical lower state energies were calculated for this region using a rearranged version of the line intensity equa-

Table 3
Total number of lines obtained at each temperature and pressure.

Temperature (K)	Lines at 10 Torr	Lines at 100 Torr
293	10,306	5426
400	9594	6070
500	8715	7232
600	8293	8615
700	7783	9229
800	6838	9418
900	7698	9809

tion,

$$\frac{S'}{S'_0} = \frac{Q_0}{Q}\exp\left(\frac{E''}{kT_0} - \frac{E''}{kT}\right)\left[\frac{1-\exp\left(-\frac{h\nu_{10}}{kT}\right)}{1-\exp\left(-\frac{h\nu_{10}}{kT_0}\right)}\right]$$

where S' is the line strength, ν_{10} is the line frequency, h is the Planck constant, Q is the internal partition function, E'' is the lower state energy, k is the Boltzmann constant, T is the temperature and where S'_0, Q_0 and T_0 refer to the line intensity, internal partition function and temperature of the reference measurement, respectively [25]. The partition function used, the values of which are detailed in Table 4, is an updated NH_3 partition function from Sousa-Silva et al. [27]. The lower state energies were obtained as described by Hargreaves et al. [25].

Table 4
Partition function for NH_3.

Temperature (K)	Partition function
293	1689.3
400	2778.5
500	4081.7
600	5742.9
700	7860.3
800	10,550.0
900	13,951.0

The experimental lower state energies obtained are presented in Fig. 5 along with HITRAN values. From Fig. 5 it is clear that our work adds substantially to the measured bands of NH_3 in the near infrared. The BYTe theoretical line list extends up to 12,000 cm^{-1}, however the accuracy in line position in this region is poor with a claimed accuracy above 5000 cm^{-1} of only 5 cm^{-1} [28]. As illustrated by Coles et al. [23], the line positions and the line intensities of the new CoYuTe line list are much improved in this region compared to BYTe. The 14 line lists obtained from this work are provided, at each temperature and for both pressures, in the supplementary material. For each observed line they contain line position, line strength and lower state energy if a calculation was possible. The mean difference in line position amongst all matched lines after calibration is 4.8 $\times$ 10^{-4} cm^{-1} for the 10 Torr list and 5.5 $\times$ 10^{-4} cm^{-1} for the 100 Torr list. The accuracy of the intensities is also estimated by comparison with matched HITRAN lines (after calibration). The mean difference of the matched lines is within 20%.

The empirical lower state energies of the lines shown with the lower state energies from HITRAN in Fig. 5 demonstrate the large number of missing ammonia lines in this region in the HITRAN database. The typical parabolic P and R branches can be seen in most of the bands; however, the central Q branches are not clear. The accuracies of the experimental lower state energies are relatively low and should be used only as a guide for spectroscopic assignments. Given that many of the weaker lines were measured at the higher pressure with reduced accuracy, care should be taken when using the lower state energies. They are however appropriate for use in extrapolation of the line intensity to nearby temperatures for the intended use in the study of hot astronomical objects.

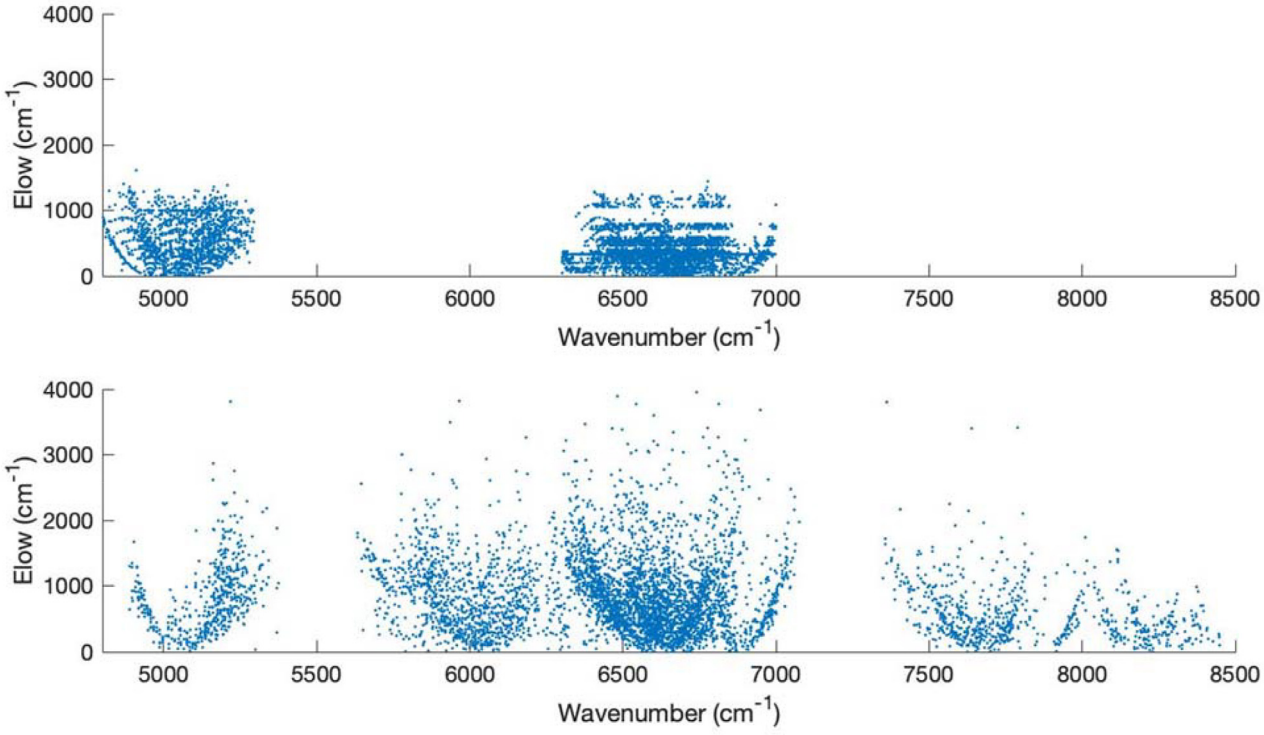

Fig. 5. Experimentally derived lower state energies (lower), compared to HITRAN (upper) values. Note the lack of coverage in the HITRAN database throughout this region.

4. Conclusions

High resolution transmission spectra of ammonia have been recorded at seven temperatures between 293 K and 900 K in the 4800–9000 cm^{-1} region. The HITRAN molecular database is particularly sparse in this region. This work provides a significant number of new lines from many overtone, combination and hot bands in the near infrared. Line lists are provided that include calibrated line positions, intensities and experimentally estimated lower state energies, extending our previous ammonia line lists [17-19]. These results can be used to model ammonia in the atmospheres of exoplanets and brown dwarfs at high temperatures.

Declaration of Competing Interests

The authors declare that they have no known competing financial interests or personal relationships that could have appeared to influence the work reported in this paper.

CRediT authorship contribution statement

Christopher A. Beale: Data curation, Formal analysis, Writing - original draft. **Andy Wong:** Data curation. **Peter Bernath:** Project administration, Funding acquisition, Supervision, Writing - original draft.

Acknowledgements

Support was provided by the NASA Laboratory Astrophysics Program.

Supplementary material

Supplementary material associated with this article can be found, in the online version, at doi:10.1016/j.jqsrt.2020.106911.

References

[1] Krupa SV. Effects of atmospheric ammonia (NH_3) on terrestrial vegetation: a review. Environ Pollut 2003;124:179–221. doi:10.1016/S0269-7491(02)00434-7.
[2] Pearson J, Stewart GR. The deposition of atmospheric ammonia and its effects on plants. New Phytol 1993;125:283–305. doi:10.1111/j.1469-8137.1993.tb03882.x.
[3] Kirkby JC. Role of sulphuric acid, ammonia and galactic cosmic rays in atmospheric aerosol nucleation. Nature 2001;476:429–33. doi:10.1038/nature10343.
[4] Ho PTP, Barrett AH, Meyers PC, Matsakia DN, Cheung AC, Chui MF, et al. Ammonia observations of the Orion molecular cloud. Astrophys J 1979;234:912–21. doi:10.1086/157575.
[5] Ho PTP, Townes CH. Interstellar ammonia. Annu Rev Astron Astrophys 1983;21:239–70. doi:10.1146/annurev.aa.21.090183.001323.
[6] Wu Y, Zhang Q, Yu W, Miller M, Mao R, Sun K, Wang Y. Ammonia cores in high mass star formation regions. Astron Astrophys 2006;450:607–16. doi:10.1051/0004-6361:20053203.
[7] Saumon D, Marley MS, Cushing MC, Leggett SK, Roellig TL, Lodders K, et al. Ammonia as a tracer of chemical equilibrium in the T7.5 dwarf Gliese 570D. Astrophys J 2006;647:552–7. doi:10.1086/505419.
[8] Carlson R, Smythe W, Baines K, Barbinis E, Becker K, Burns R, et al. Near-infrared spectroscopy and spectral mapping of Jupiter and the Galilean satellites: results from Galileo's initial orbit. Science 1996;274:385–8. doi:10.1126/science.274.5286.385.
[9] Fletcher LN, Swinyard B, Salji C, Polehampton E, Fulton T, Sidher S, et al. Submillimetre spectroscopy of Saturn's trace gases from Herschel/SPIRE. Astron Astrophys 2012;539:A44. doi:10.1051/0004-6361/201118415.
[10] Nelson RM, Kamp LW, Matson DL, Irwin PGJ, Baines KH, Boryta MD, et al. Saturn's Titan: surface change, ammonia, and implications for atmospheric and tectonic activity. Icarus 2009;199:429–41. doi:10.1016/j.icarus.2008.08.013.
[11] MacDonald RJ, Madhusudhan N. HD 209458b in new light: evidence of nitrogen chemistry, patchy clouds and sub-solar. Mon Not R Astron Soc 2017;469:1979–96. doi:10.1093/mnras/stx804.
[12] Burrows A, Hubbard WB, Lunine JI, Liebert J. The theory of brown dwarfs and giant planets. Rev Mod Phys 2001;73:719–65. doi:10.1103/RevModPhys.73.719.
[13] Cushing MC, Roellig TL, Marley MS, Saumon D, Leggett SK, Kirkpatrick JD, et al. A Spitzer infrared spectrograph spectral sequence of M, L, and T dwarfs. Astrophys J 2006;648:614. doi:10.1088/0004-637X/706/1/923.
[14] Brown LR, Margolis JS. Empirical line parameters of NH_3 from 4791 to 5294 cm^{-1}. J Quant Spectrosc Radiat Transf 1996;56:283–94. doi:10.1016/0022-4073(96)00041-6.
[15] Cermak P, Hovorka J, Veis P, Cacciani P, Cosléou J, Romh JE, et al. Spectroscopy of $^{14}NH_3$ and $^{15}NH_3$ in the 2.3 μm spectral range with a new VECSEL laser source. J Quant Spectrosc Radiat Transf 2014;137:13–22. doi:10.1016/j.jqsrt.2014.01.005.
[16] Kleiner I, Brown LR, Tarrago G, Kou QL, Picqué N, Guelachvili G, et al. Positions and intensities in the $2\nu_4/\nu_1/\nu_3$ vibrational system of $^{14}NH_3$ near 3 μm. J Mol Spectrosc 1999;193:46–71. doi:10.1006/jmsp.1998.7728.
[17] Hargreaves RJ, Li G, Bernath PF. Hot NH_3 spectra for astrophysical applications. Astrophys J 2011;735:111. doi:10.1088/0004-637X/735/2/111.
[18] Hargreaves RJ, Li G, Bernath PF. Ammonia line lists from 1650 to 4000 cm^{-1}. J Quant Spectrosc Radiat Transf 2012;113:670–9. doi:10.1016/j.jqsrt.2012.02.033.
[19] Beale CA, Hargreaves RJ, Coles P, Tennyson J, Bernath P. Infrared absorption spectra of hot ammonia. J Quant Spectrosc Radiat Transf 2017;203:410–16. doi:10.1016/j.jqsrt.2017.02.012.
[20] Huang X, Schwenke DW, Lee TJ. Rovibrational spectra of ammonia. I. Unprecedented accuracy of a potential energy surface used with nonadiabatic corrections. J Chem Phys 2011;134:044320. doi:10.1063/1.3541351.
[21] Huang X, Schwenke DW, Lee TJ. Rovibrational spectra of ammonia. II. Detailed analysis, comparison, and prediction of spectroscopic assignments for $^{14}NH_3$, $^{15}NH_3$, and $^{14}ND_3$. J Chem Phys 2011;134:044321. doi:10.1063/1.3541352.
[22] Yurchenko SN, Barber RJ, Tennyson J. A variationally computed line list for hot NH_3. Mon Not R Astron Soc 2011;413:1828–34. doi:10.1111/j.1365-2966.2011.18261.x.
[23] Coles PA, Yurchenko SN, Tennyson J. ExoMol molecular line lists – XXXV. A rotation-vibration line list for hot ammonia. Mon Not R Astron Soc 2019;490:4638–47. doi:10.1093/mnras/stz2778.
[24] Gordon IE, Rothman LS, Hill C, Kochanov RV, Tan Y, Bernath PF, et al. The HITRAN 2016 molecular spectroscopic database. J Quant Spectrosc Radiat Transf 2017;203:3–69. doi:10.1016/j.jqsrt.2017.06.038.
[25] Hargreaves RJ, Bernath PF, Bailey J, Dulick M. Empirical line lists and absorption cross sections for methane at high temperatures. Astrophys J 2015;813:12. doi:10.1088/0004-637X/813/1/12.
[26] Carleer M.R. WSpectra: a windows program to accurately measure the line intensities of high-resolution Fourier transform spectra. Proceedings of the SPIE 4168, remote sensing of clouds and the atmosphere V 2001:337. DOI: 10.1117/12.413851.
[27] Sousa-Silva C, Hesketh N, Yurchenko SN, Hill C, Tennyson J. High temperature partition functions and thermodynamic data for ammonia and phosphine. J Quant Spectrosc Radiat Transf 2014;142:66–74. doi:10.1016/j.jqsrt.2014.03.012.
[28] Polyansky OL, Ovsyannikov RI, Kyuberis AA, Lodi L, Tennyson J, Yachmenev A, et al. Calculation of rotation-vibration energy levels of the ammonia molecule based on an ab initio potential energy surface. J Mol Spectrosc 2016;327:21–30. doi:10.1016/j.jms.2016.08.003.